2×2 TeV $\mu^+\mu^-$ Collider

N. V. Mokhov and R. J. Noble
Fermi National Accelerator Laboratory
P.O. Box 500, Batavia, Illinois 60510, U. S. A.

1. Introduction

The possibility of muon colliders was introduced by Skrinsky et al. [1] and Neuffer [2]. More recently, several workshops and collaboration meetings (see, e. g., [3]) have greatly increased the level of understanding. After the workshop at Sausalito in December 1994, a collaboration was formed by BNL, FNAL and LBL to study the concept and prepare a document for the 1996 Snowmass meeting [4]. This paper reviews briefly the main features of the project as well as the progress made since the Snowmass meeting.

Hadron collider energies are limited by machine size, and technical constraints on the magnetic bend fields. Lepton colliders in general, offer the advantage that the interaction energy is given by twice the machine energy, because they undergo simple, single-particle interactions, compared to hadron colliders where the effective energy is much lower than that of the proton. Even worse, the gluon-gluon background radiation makes it increasingly difficult to sort out the complicated decay schemes envisaged for the SUSY particles. A lepton collider on the other hand offers clean production of charged pairs with a cross section comparable to $\sigma_{\rm QCD} = 100/s$ fb where s is the center-of-mass (CM) energy squared in TeV^2.

Extension of e^+e^-colliders to multi-TeV energies is severely performance-constrained by beamstrahlung, and cost-constrained because two full energy linacs are required to avoid the excessive synchrotron radiation that would occur in rings. Muons ($\frac{m_\mu}{m_e} = 207$) have the same advantage in energy reach as electrons, but have negligible beamstrahlung, and can be accelerated and stored in rings with a much smaller radius than a hadron collider of comparable energy reach, making the possibility of high-energy $\mu^+\mu^-$colliders attractive.

There are many detailed particle reactions which are open to a muon collider. Most of the physics accesible to an e^+e^-collider could be studied in a $\mu^+\mu^-$machine. In addition the production of Higgs bosons in the s-channel will allow the measurement of Higgs masses and total widths to high precision; likewise, $t\bar{t}$ and W^+W^- threshold studies would yield m_t and m_W to great accuracy. These reactions are at low CM energy (if the minimal supersymmetric Standard Model is correct) and the luminosity and $\Delta p/p$ of the beams required for these measurements is detailed in [4]. On the other hand, at 2×2 TeV, a luminosity of $\mathcal{L} \sim 10^{35}\,{\rm cm}^{-2}\,{\rm s}^{-1}$ is desirable for studies such as, the scattering of longitudinal W bosons or the production of heavy scalar particles.

Naturally, one would, if the concept is shown to be of interest, initially construct a lower energy $\mu^+\mu^-$collider, e. g., 250×250 GeV [4, 5]. Such a machine with a luminosity of $\mathcal{L} \sim 10^{33}\,{\rm cm}^{-2}\,{\rm s}^{-1}$ could serve as a prototype for exploring the properties and technologies needed for this class of colliders, while providing useful physics.

2. Basic Description of the Machine

The $\mu^+\mu^-$collider complex consists of components (see Fig. 1) which first produce copious pions, then capture the pions and the resulting muons from their decay; this is followed by an ionization cooling channel to reduce the longitudinal and transverse emittance of the muon beam. The next stage is to rapidly accelerate the muons and, finally, inject them into a collider ring which has a small β-function at the colliding point. Table 1 shows the main parameters for the low-energy and high-energy $\mu^+\mu^-$colliders. The normalized emittance is defined as $\epsilon^N = \beta\gamma\epsilon$, where the emittance ϵ is *rms* transverse phase space area divided by π.

Table 1: Parameters of high luminosity $\mu^+\mu^-$colliders

		4 TeV	0.5 TeV
Beam energy	TeV	2	.25
Beam γ		19,000	2,400
Repetition rate	Hz	15	15
Muons per bunch	10^{12}	2	4
Bunches of each sign		2	1
Normalized *rms* emittance ϵ^N	$10^{-6}\pi$ m $-$ rad	50	90
Bending Field	T	9	9
Circumference	km	7	1.2
Average ring mag. field B	T	6	5
Effective turns before decay		900	800
β^* at intersection	mm	3	8
rms beam size at I.P.	μm	2.8	17
Luminosity	$\mathrm{cm}^{-2}\mathrm{s}^{-1}$	10^{35}	5×10^{33}

3. Proton Source, Pion Production and Phase Rotation

The proton driver is a rapid cycling synchrotron used for pion production. Table 2 shows parameters for a candidate 30 GeV proton driver. Lower energy (8 – 10 GeV) drivers have also been considered in [4]. A high intensity proton bunch is compressed and focussed on a pion production target. The pions generated are captured by a high field solenoid and transferred to a solenoidal decay channel within a low frequency linac (Fig. 2). The linac serves to reduce, by phase rotation, the momentum spread of the pions and of the muons into which they decay.

The target studies [6] using the MARS code [7] show that while a 1 to 2 λ_I copper target is optimum for yield, lower–Z targets are not much worse—about 20% depending on the collection geometry for 8 GeV protons (Fig. 3). Hence lower–Z targets, because of the lower energy deposition associated with them, may still be the targets of choice. A 30 GeV proton beam is not preferred on the basis of yield per megawatt of power deposited in the target, but may be needed to make short (1 nsec) bunches. The use of tritons instead of protons at the same momentum can increase pion yield per projectile on target by up to a factor of two.

Table 2: Proton driver requirements; target and particle production parameters; capture and transfer solenoid system

Energy [GeV]	30
Rep. Rate [Hz]	15
Protons [/pulse]	10^{14}
Bunches [@ target]	4
Protons [/bunch]	2.5×10^{13}
σ_t [ns]	1
P_{beam} [MW]	7.2
ϵ_{Nrms}, 10^{-6} [m-rad]	40
β_{target} [m]	12
$\sigma(x)$ [mm]	4
$\sigma(x')$ [mrad]	0.3
B_{sol} [T]	20
a_{sol} [cm]	7.5
$p_{\perp max}$ [GeV/c]	0.225
A_N [m-rad]	0.12
L_{target} [cm]	22.5
r_{target} [cm]	1
$\pi^{\pm}/p$	1.2
P on target [kW]	600
Nominal Transport Magnetic Induction [T]	5.0
Stored Magnetic Energy to x = 3 meters [MJ]	37.9
Stored Energy S/C Magnet to x = 3 meters [MJ]	22.4
Stored Energy for x > 3.0 meters [MJ/m]	1.58

Target heating is very severe in high–Z materials at 30 GeV (Fig. 3). Spreading the beam diameter to a large fraction of the solenoid bore generally helps by lowering the average heating power density and the shock energy density deposition. A variety of configurations appear to satisfy the steady-state heat removal target requirements. Microchannel cooling, large diameter beams and targets or recirculating liquid targets may be used to deal with the severe target heating problems in high–Z targets. Solid carbon targets however are still workable with adequate cooling. Lower energy proton beams at lower repetition rates (*e.g.*, 8 GeV, 15 Hz) would help reduce target powers substantially.

Quenching due to energy deposition in superconducting solenoids near the target is a problem only for high-field/small-diameter magnets and high–Z targets. Lower field solenoids with larger diameter are much less likely to quench and also pose less technological difficulties. The simulations confirm the superiority of muon collection with the solenoid scheme versus lithium lenses and quadrupoles in this proton energy regime. Considerations of π/μ decay indicate a collection limit of about 0.95 muons per pion. Total yields of 0.5 to 1 muons per proton of either charge appear to be obtainable. Kaons appear to contribute far less than their numbers to the usable muon flux and are practically negligible in this application. The pion momentum spectrum after the target generated by either 8 GeV or 30 GeV protons peaks in the range 0.2 to 0.3 GeV/c. The collection system with phase rotation tends to favor the lower energies and most muons are expected to be in the 0.2 to 0.5 GeV/c range. Charge separation by *curved* solenoids practically

doubles the number of muons collected and appears to be beneficial in disposing of the host of unwanted particles generated in the target along with the through-going proton beam.

4. Ionization Cooling

In order to generate sufficient muons for the collider, it is necessary to capture a very large fraction of the pions created at the target. These pions, and the muons into which they decay, are then necessarily very diffuse (i.e. they have a very large emittance). In order to achieve the required luminosity of $10^{35} cm^{-2}\, s^{-1}$ at $2 \times 2\,\mathrm{TeV}$, it is necessary to reduce the transverse emittance by a factor of ≈300 in each plane and the longitudinal emittance by a factor of ≈10. Therefore, it is essential to provide some means for for cooling the muon beams.

The large mass of the muon compared to that of the electron prevents cooling by radiation damping, while the short lifetime of the muon prevents conventional stochastic or electron cooling. Fortunately, the process of ionization cooling [2], which because of their long interaction length is possible only for muons, can be used. In this process the muon loses transverse and longitudinal momentum by electron collisions in a material and then has the longitudinal momentum (but not the transverse momentum) restored in a subsequent RF cavity (Fig. 4). The combined effect is to reduce the beam divergence and thus the emittance of the beam. The use of wedge absorbers in dispersive regions permits longitudinal cooling. The overall process is complicated by the simultaneous presence of multiple scattering in the material, which acts as a source of *heat* and increases the emittance. The cooling effect can dominate for low–Z materials in the presence of strong focussing fields. One solution being considered for the collider is to use absorbers made of lithium, beryllium, or liquid hydrogen in a lattice of solenoid magnets or quadrupole arrays. The absorber provides the energy loss, while the large aperture magnets provide the required focussing. Model cooling systems have been studied with differential equations (Fig. 5), and multiparticle simulation codes are now under development [8]. Table 3 contains parameters for a possible cooling scheme taken from [4].

Table 3: Cooling section summary

total length		903	m
sections		23	
total acceleration		5.3	GeV
accelerator length		826	m
μ decay loss		49	%
contingency loss		20	%
	Entrance	Exit	
KE	300	15	MeV
p	392	58	MeV/c
ϵ_{xN}(rms)	15000	44	mm mr
ϵ_{zN}(rms)	63	11	m %
σ_z	1.55	0.65	m
$\frac{\delta p}{p}$	11.0	31.2	%
μ intensity	7.5	3.0	10^{12} / bunch

5. Muon Acceleration

The acceleration system must take beam from the cooling system to full energy. Muons must be accelerated to the desired energy before significant decay occurs. The muon lifetime is 2.2 μsec at rest but increases with energy. If the average acceleration gradient in the complex exceeds a MV/meter, muon survival will be 50 % or more at TeV final energies [9]. In the cooling section, the initial muons are collected, cooled, and pre-accelerated into moderately compact μ^+ and μ^- bunches at $E_\mu \approx 1$ GeV. Studies of the cooling system indicate that an rms energy spread of ≈ 1.5 % with a bunch length of ≈ 25 cm at 1 GeV are reasonable design goals. The accelerator must accelerate these bunches to 2 TeV and transfer them into the collider, which requires a final energy spread of ≈ 0.1 % and a bunch length reduced to ≈ 0.3 cm. These collision requirements set the longitudinal phase-space area of the beam at collisions at ≈ 3 mm $\times$ 2 GeV ($\frac{\Delta E}{E} = 0.001$ for 2 TeV), or 0.02 eV-s, which is not much larger than the beam emittance at the beginning of the acceleration. The cooling system also reduces the normalized transverse emittance to a design value of $\epsilon_N \approx 0.25 \times 10^{-4}$ m-rad. The acceleration system must accelerate this beam to full energy while maintaining an emittance of $\epsilon_N < 0.5 \times 10^{-4}$ m-rad. The design intensity is 2×10^{12} μ's per bunch, which is a relatively high charge per bunch (larger than existing accelerators). The acceleration system must accommodate these intense bunches. Wakefield and beam loading effects can become important, particularly in the higher-energy end of the accelerator, where bunch-lengths are reduced toward 0.3 cm, obtaining high-peak currents. The preferred acceleration scenario is a set of four CEBAF-like recirculating linacs (RLA) accelerating muons for about 10 turns each up to 10, 70, 250 and 2000 GeV, respectively. Rapid-cycling synchrotrons and hybrid schemes are also under consideration.

6. Muon Collider Ring

The collider ring of the Muon Complex allows for 1000-2000 collisions per bunch, rather than the single collision that is possible in a linear collider geometry. The muon bunch is cooled as much as possible, but still has an emittance that is significantly larger than the extremely low emittances required in an e^+e^-linear collider. The muon collider has two μ^+ and two $\mu-$ bunches with N=2×10^{12} each, a round beam with ϵ_n=5×10^{-5} m rad and β^*=3×10^{-3} m, for a luminosity of 10^{35} cm^{-2} s^{-1} at 2 × 2 TeV. The $\mu^+\mu^-$collider achieves its luminosity primarily with an increased number of particles and from an increased number of collisions per bunch-pair compared to a single-pass linear collider. Table 1 contains the principal collider parameters for 0.5 and 4 TeV CM energies. Higher luminosity could be achieved with more particles per bunch, but the beam-beam interaction ultimately dilutes emittance and leads to luminosity loss (Fig. 6). The intensity in the muon accelerator however is limited to about 3×10^{12} muons per bunch due to RF beam loading effects in the superconducting cavities.

The collider will be a single separated-function ring of superconducting magnets that guides both the negative and the positive muons. The lattice for at 2 × 2 TeV $\mu^+\mu^-$collider must satisfy three major design constraints. The first and most difficult of these is provision of an interaction region (IR) with an extremely low β^* ($\sim$ 3 mm) consistent with an acceptable dynamic aperture. Second, the ring must exhibit a high degree of isochronicity in order to preserve short 3 mm long bunches with a modest RF system. Lastly, there

must be small corrected chromaticity, so that the momentum-dependent tune spread of the beam fits between resonances. In existing lattice designs the maximum β-function reaches 200 km, so the design of very high gradient superconducting quadrupoles for the final focus with the inner coil diameter of 25–30 cm is a challenging problem. From the behavior of the chromaticity and amplitude-dependent tunes with momentum spread, the momentum aperture $\Delta p/p$ of the lattice is an acceptable 0.007. Recent improvements since the Snowmass meeting have also improved the dynamic aperture of the lattice to about five sigma.

Considerable shielding must be incoporated into the design to protect the superconducting magnets from the high muon-decay backgrounds. Table 4 from [4] presents calculations for muon decay in each of the accelerator components and the collider ring. Included in the Table is the number of turns through the component and the total transit length L_T through the structure. Table 4 gives an estimate of the decayed muon power that is transferred to electrons and positrons which can end up in the superconducting magnet system. Several design approaches have been considered to solve the problem. The MARS calculations [4, 10] show that the thickness of tungsten needed to reduce the heat load from decay by three orders of magnitude is about 65 mm, cooled at nitrogen or room temperatures. Taking into account the fact that most of the power from decays and induced electromagnetic showers is deposited in the mid-plane, a design with cold or warm iron and coils completely separated on the mid-plane is much more attractive (Fig. 7).

Table 4: Muon decay parameters a muon collider complex

Component	Peak Energy (GeV)	Number of Turns	L_T(km)	Total Muon Decay Rate $10^{13}s^{-1}$	Heating Power (kW)	Peak Heat per unit L (Wm^{-1})
Linac	1.0	-NA-	0.12	1.9	0.6	-NA-
First Ring	9.6	9	2.17	1.2	3.6	1.64
Second Ring	79	12	11.3	0.8	19.7	1.75
Third Ring	250	18	29.2	0.4	36.8	1.26
Fourth Ring	2000	18	227	0.6	378	1.66
Collider Ring	2000	1000	7.9	13.1	14600	1840

7. Detector Background

A third of the muon beam power released in the machine components via electromagnetic and hadronic showers results in high heat load to cryogenics (see above), induces radiation levels in the machine and surroundings and creates the enormous background particle fluxes in the detector components. With 2×10^{12} muons in a bunch at 2 TeV one has 2×10^5 $\mu \to e\nu\tilde{\nu}$ decays per meter in a single pass through an interaction region, or 6×10^9 decays per meter per second. Decay electrons with an energy of about 700 GeV and the huge number of synchrotron photons emitted by these electrons in a strong magnetic field induce electromagnetic showers in the collider and detector components. Detailed calculations [4, 10, 11, 12] have shown that the resulting particle fluxes can exceed those at hadron colliders and have the potential of killing the concept of the muon collider

without significant suppression via appropriate IR design, shielding and collimators in the detector vicinity.

It was found that a careful design of the final focus system with tapered apertures, dipole magnets interspersed with collimators and tungsten collimators having the aspect of two nozzles inside the detector can reduce the background levels by several orders of magnitude. Fig. 8 shows an effect of spraying the decay electrons along the final focus region and corresponding reduction in photon flux in the detector for the latest IR design. The power dissipation in the IR quadrupoles is reduced from a few kW per meter to 1–5 W/m compared to earlier configurations. But even with this one has a few thousand photons and neutrons and a few tens of charged particles (mainly $e^{\pm}$, $\pi^{\pm}$ and $\mu^{\pm}$) per cm^2 of inner tracker per each bunch crossing (every $20\,\mu$sec), so more work is obviously needed.

Another contribution to the background comes from beam loss at the limiting apertures. There will need to be a very efficient scraping system to catch beam halo on the far-side of the collider ring.

8. Radiation Issues

All aspects of radiation control at a $\mu^+\mu^-$ collider complex are folded into the design. Considered in detail in [4, 13] are the main collider arcs, the IR and absorption of spent muon beam for operational and accidental cases. Prompt and residual radiation levels have been calculated with the MARS code. In the tunnel, experimental hall and in the first meters of the surrounding soil/rock, the prompt radiation field is composed of low energy photons and neutrons. Farther from the tunnel the only significant component is muons generated in electromagnetic and hadronic cascades in the magnets. Fig. 9 shows isodose contours around the collider tunnel. The distributions are asymmetric in the horizontal plane because of lattice and tunnel curvature and effects of the magnetic field. With 10^7 s as a collider operational year, the tolerable on-site limit in the soil/rock is reached at about 6 m above the orbit plane, 10 m toward the ring center and ~ 75 m outward in the horizontal plane. In calculations the ^{3}H and ^{22}Na radionuclide production is observed in the first meters of the soil/rock around the tunnel, which would require insulation or drainage of that region. The dolomite stratum at Fermilab may naturally satisfy this condition. Residual dose rates in magnet components immediately after shutdown range from ~ 10 rad/hr (innermost radii) to ~ 0.003 rad/hr at the magnet outer shell.

After about 1000 turns muons are extracted and sent to a beam absorber. For 2 TeV muons the isodose contour coinciding with the tolerable on-site dose limit is 3.55 km long with a maximum width of 18 m at 2.6 km. Deflecting the extracted beam down by 4.5 mrad confines muon fluxes beneath the ground. Estimates show that the absorption of the spent beam can result in annual activity concentration which may exceed the stringent limits for ^{3}H and ^{22}Na radionuclides, 20 pCi/cm^3 and 0.2 pCi/cm^3 respectively, if the beam disposal lines are in aquiferous layers. The problem is solved if the 2 TeV beam is directed into the impervious dolomite layer or to an isolated 2.5 km long 2 m radius rock or concrete plug. For 250 GeV beam this plug is about 550 m long and 1 m in radius.

9. Conclusion

The one and a half year feasibility study of the muon collider that lead to the Snowmass report [4] indicates that the concept probably has no fundamental flaws. However, its realization may be 15 or more years away, and it will certainly be the most technically challenging high-energy machine ever built. A $\mu^+\mu^-$ collider would enable multi-TeV physics to be done early in the next century with circular machines that would fit on the existing Fermilab site. The collaboration study group that produced the Snowmass report is continuing with a more detailed study over the next year. The efficient production of polarized muons is one of the outstanding issues. Polarization is very desireable at TeV energies to disentangle the physics of possible supersymmetric particles with different spins. In addition detailed simulations of muon ionization cooling will be carried out to achieve a self-consistent scenario which could then lead to the definition of an experimental cooling project at Fermilab in 2 or 3 years. Further studies are underway to mitigate the detector background problem and to begin an extensive design and optimization program for components.

Acknowledgments

The work described in this paper reflects the efforts of many people in the $\mu^+\mu^-$ Collider Study collaboration whose names and contributions are found in [4]. The authors gratefully acknowledge their work.

Fermilab is operated by the Universities Research Association, Inc., under contract DE-AC02-76CH00300 with the U. S. Department of Energy.

References

[1] E. A. Perevedentsev and A. N. Skrinsky. *Proc. 12th Int. Conf. on High Energy Accelerators*, F. T. Cole and R. Donaldson. Eds., 485 (1983); A. N. Skrinsky and V. V. Parkhomchuk.
Sov. J. Nucl. Physics **12**, 3 (1981).

[2] D. Neuffer. 'Colliding Muon Beams at 90 GeV', Fermilab–FN–319 (1979); D. Neuffer. Particle Accelerators, **14**, 75 (1983); D. Neuffer. *Proc. 12th Int. Conf. on High Energy Accelerators*, F. T. Cole and R. Donaldson. Eds., 481 (1983).

[3] 'Physics Potential and Development of $\mu^+\mu^-$ Colliders'. Sausalito-94, ed. by D. Cline, *AIP Conference Proceedings* **352** (1996).

[4] '$\mu^+\mu^-$ Collider: A Feasibility Study'. The $\mu^+\mu^-$ Collider Collaboration, BNL–52503; Fermilab–Conf–96/092; LBNL–38946, July 1996.

[5] R. B. Palmer, A. Sessler and A. Tollestrup. 'Progress on the Design of a High Luminosity $\mu^+\mu^-$ Collider', BNL–63245, June 1996.

[6] N. V. Mokhov, R. J. Noble and A. Van Ginneken. 'Targetry and Collection Optimization for Muon Colliders'. In: *AIP Conference Proceedings* **372**, *9th Advanced ICFA*

Beam Dynamics Workshop: Beam Dynamics and Technology Issues for $\mu^+\mu^-$ Colliders, Montauk, NY, October 15–20, 1995, pp. 61–86; also Fermilab–Conf–96/006 (1996).

[7] N. V. Mokhov. 'The MARS Code System User's Guide, Version 13(95)', Fermilab–FN–628 (1995).

[8] A. Van Ginneken (SIMUCOOL), R. Thun (private communication), R. Palmer and J. Gallardo (MUMC), H. Kirk (PARMELA), R. Fernow (ICOOL).

[9] R. J. Noble. 'Particle Production an Survival in Muon Acceleration', *Proc. of the 3rd Int. Workshop on Advanced Accelerator Concepts*, NY, AIP Conf. Proc. No. 279, 949 (1993).

[10] N. V. Mokhov and S. I. Striganov. 'Simulation of Backgrounds in Detectors and Energy Deposition in Superconducting Magnets at $\mu^+\mu^-$ Colliders', in [6] pp. 234–256; also Fermilab–Conf–96/011 (1996).

[11] G. W. Foster and N. V. Mokhov. 'Backgrounds and Detector Performance at a 2×2 TeV $\mu^+\mu^-$ Collider', in [3] pp. 178–190; also Fermilab–Conf–95/037 (1995).

[12] N. V. Mokhov. 'Comparison of Backgrounds in Detectors for LHC, NLC and $\mu^+\mu^-$ Colliders', in *Proceedings of Symposium on Physics Potential and Development of $\mu^+\mu^-$ Colliders*, San Francisco, CA, December 1995; Fermilab-Conf-96/062 (1996).

[13] N. V. Mokhov. 'The Radiation Environment at Muon Colliders'. In: *Proc. of the 2nd Workshop on Simulating Accelerator Radiation Environments (SARE2)*, CERN, Geneva, October 1995.

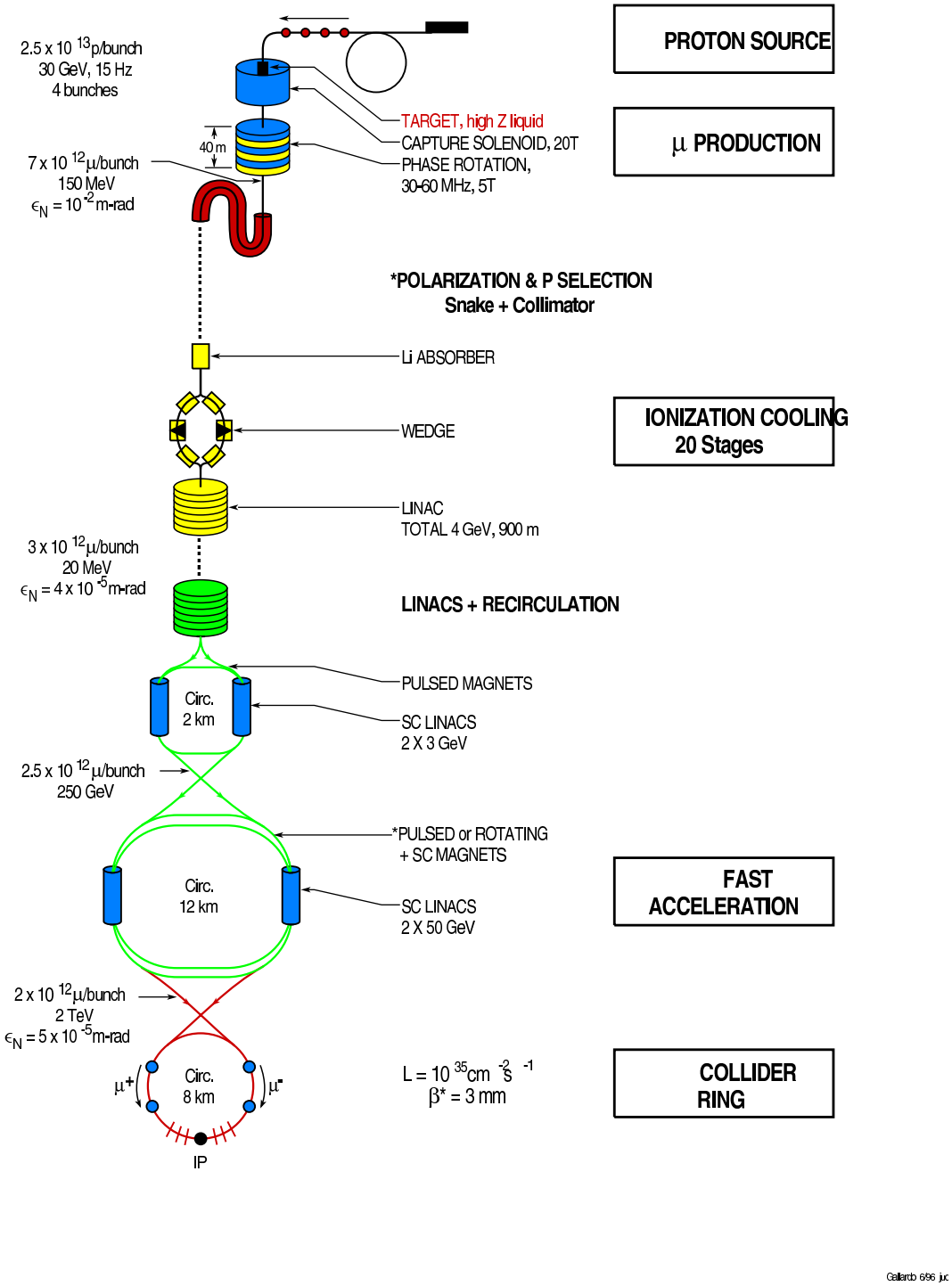

Figure 1: Schematic of a $\mu^+\mu^-$collider.

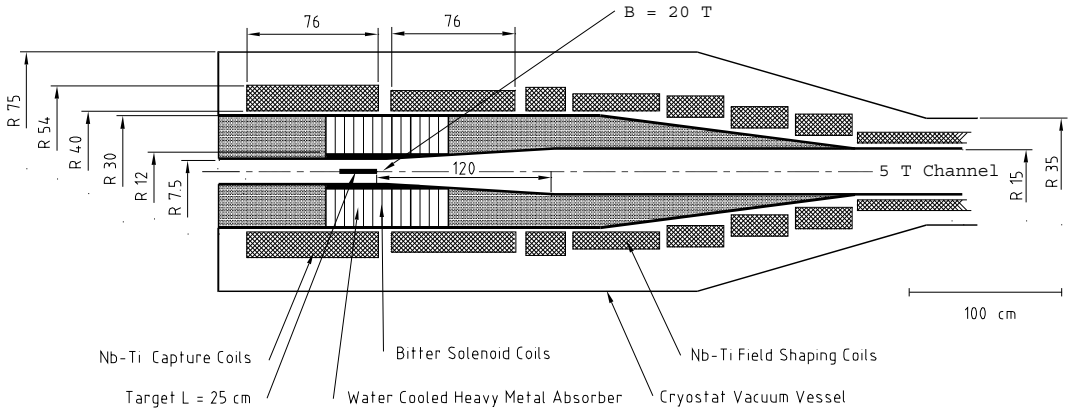

Figure 2: Capture and transfer solenoid system. Dimensions are in *cm*.

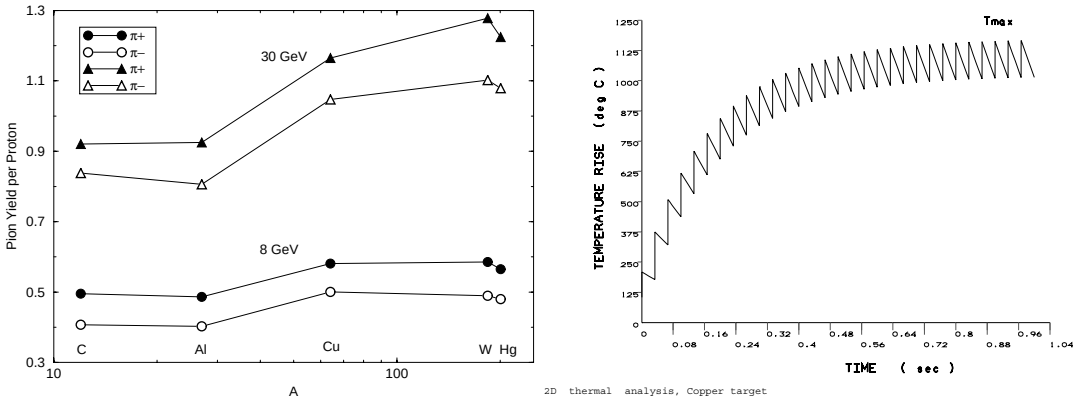

Figure 3: (a) Pion yield from $1.5\,\lambda_I$ targets of various materials at 8 and 30 GeV; (b) Maximum temperature rise a 1 cm radius $2\,\lambda_I$ long copper target irradiated by 30 GeV beam of 5×10^{13} protons at 30 Hz.

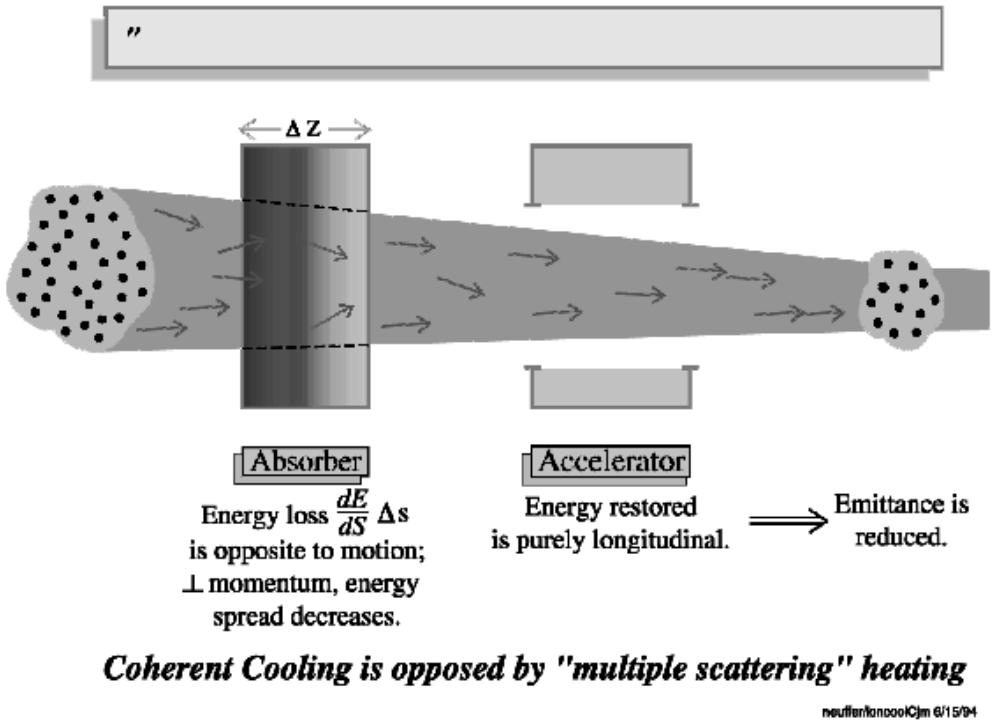

Figure 4: Basic principle of ionization cooling of transverse emittance.

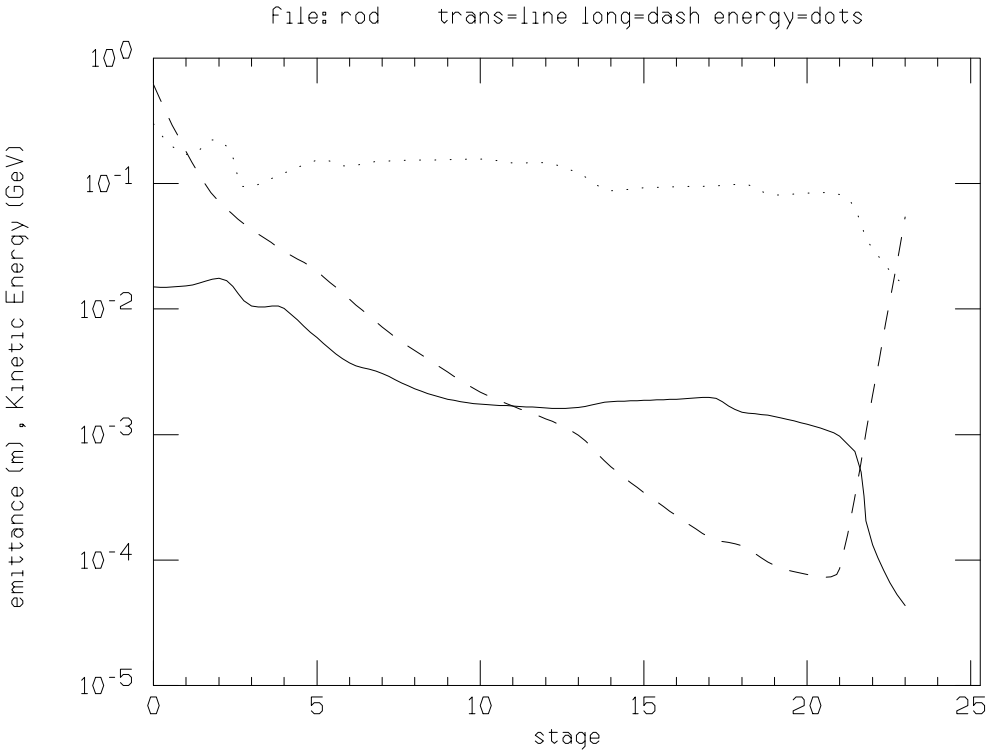

Figure 5: Normalized transverse and longitudinal emittances and muon energy as a function of section number in the model cooling system.

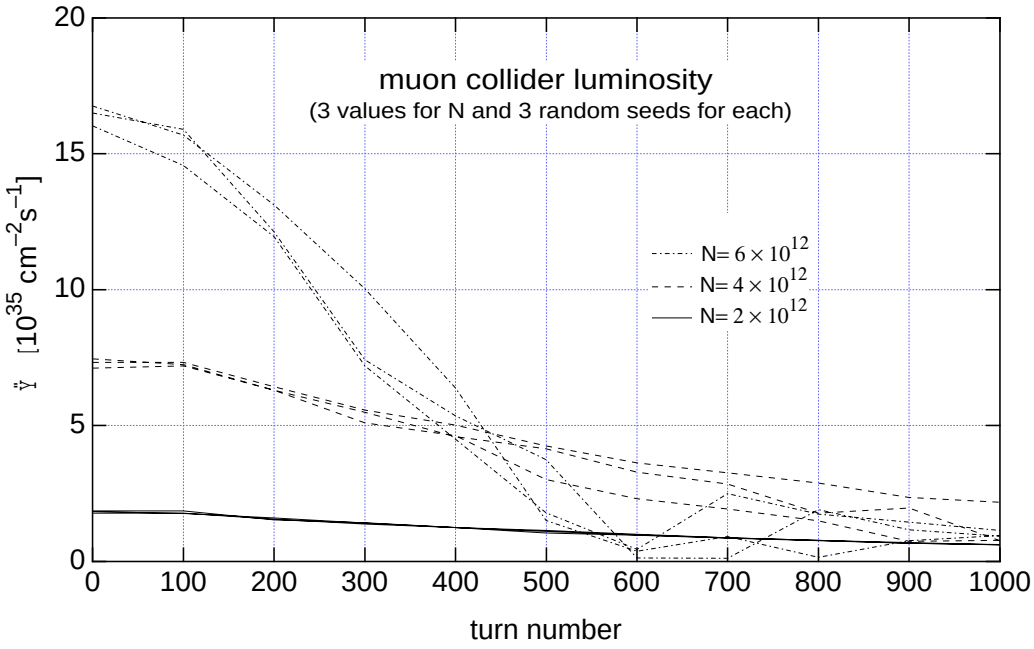

Figure 6: Luminosity as a function of turn number for three different values of the number of particles per bunch N. For each case three runs are shown, each corresponding to a different random number seed.

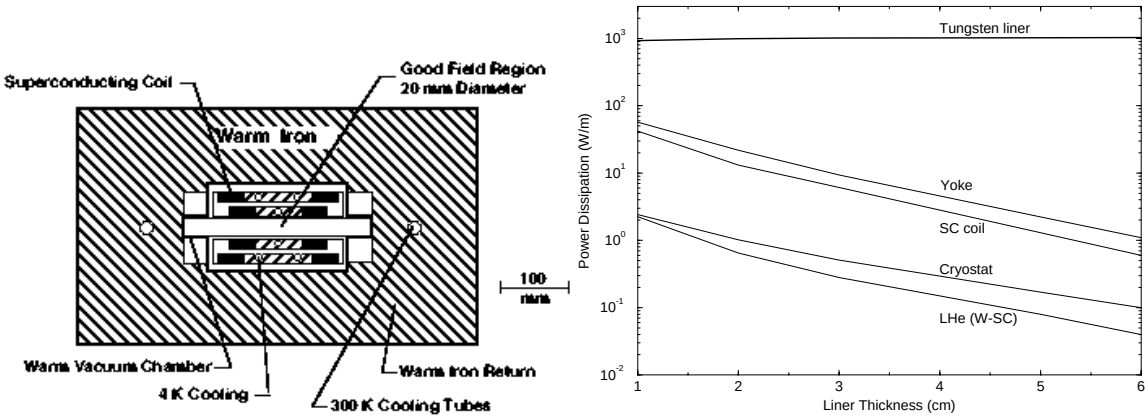

Figure 7: (a) 8.5 T dipole; (b) Power dissipation in the arc magnet components *vs* tungsten liner thickness as per MARS13(96).

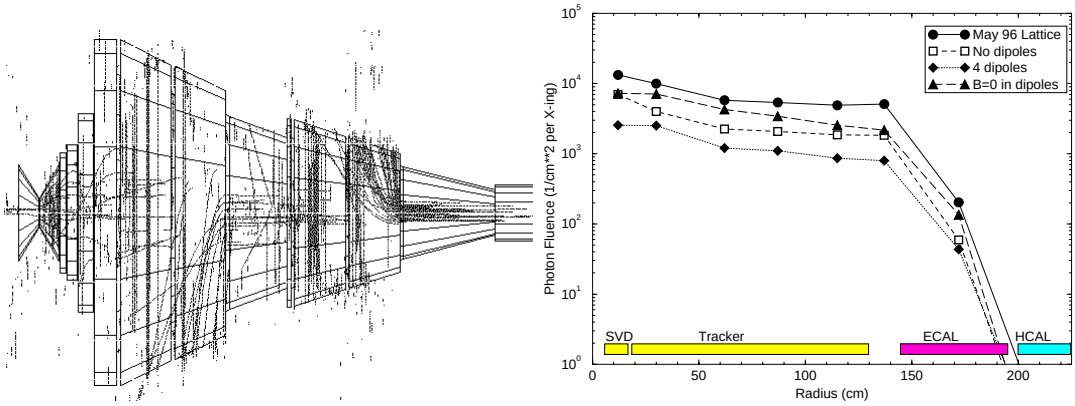

Figure 8: (a) Decay positron tracks in the IR aperture (150 m long and 10 cm radius at β_{max}); (b) Radial dependence of photon fluence in the central detector for different IR scenarios as per MARS13(96).

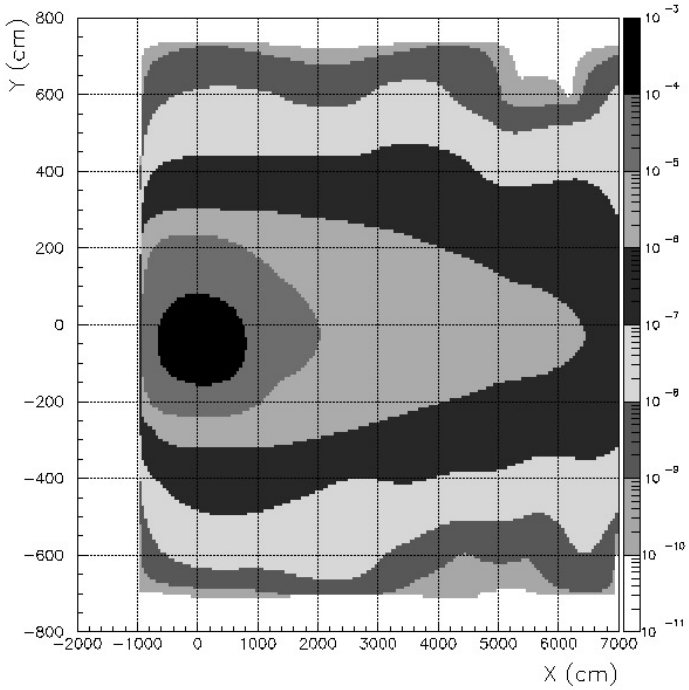

Figure 9: Isodose contours in the vertical plane across the collider tunnel and surrounding soil/rock for 2 TeV muon beam decays as per MARS13(96). y axis is up and x axis points outward along the ring radius. Beam axis is at x=y=0. Right scale is dose rate in rem/sec.